

Multi-color Optical Variability of the TeV Blazar Mrk 501 in the Low-State

A. C. Gupta¹, W. G. Deng^{2,1}, U. C. Joshi³, J. M. Bai¹ and M. G. Lee⁴

acgupta30@gmail.com, Phone No. +86 15920411403, Fax No. +86 871 3920599

Received _____; accepted _____

Submitted to New Astronomy

¹National Astronomical Observatories / Yunnan Observatory, Chinese Academy of Sciences, P.O. Box 110, Kunming, Yunnan 650011, China.

²Department of Physics, Yunnan University, Kunming, Yunnan 650091, China.

³Astronomy and Astrophysics Division, Physical Research Laboratory, Navrangpura, Ahmedabad - 380 009, India.

⁴Astronomy Program, Seoul National University, Seoul 151-742, South Korea.

ABSTRACT

We report results based on the monitoring of the BL Lac object Mrk 501 in the optical (B, V and R) passbands from March to May 2000. Observations spread over 12 nights were carried out using 1.2 meter Mount Abu Telescope, India and 61 cm Telescope at Sobaeksan Astronomy Observatory, South Korea. The aim is to study the intra-day variability (IDV), short term variability and color variability in the low state of the source. We have detected flux variation of 0.05 mag in the R-band in time scale of 15 min in one night. In the B and V passbands, we have less data points and it is difficult to infer any IDVs. Short term flux variations are also observed in the V and R bands during the observing run. No significant variation in color (B–R) has been detected but (V–R) shows variation during the present observing run.

Assuming the shortest observed time scale of variability (15 min) to represent the disk instability or pulsation at a distance of 5 Schwarzschild radii from the black hole (BH), mass of the central BH is estimated $\sim 1.20 \times 10^8 M_{\odot}$.

PACS: 98.54.Cm, 95.85.Kr, 95.75.De, 95.75.Wx

Subject headings: Optical: observations - BL Lacertae objects: individual: (Mrk 501)

1. Introduction

Blazars constitute a class of radio-loud active galactic nuclei (AGNs) consisting of BL Lacertae objects (BL Lacs) and flat spectrum radio quasars (FSRQs). In the unified schemes of AGNs, blazars are believed to be the beamed counterparts of the FR I/FR II radio galaxies and many of their properties can be well understood in such a scenario (e.g. Browne 1983; Antonucci 1993; Urry & Padovani 1995). According to orientation based unification scheme for radio-loud AGNs, blazar’s jet make angles $\leq 20^\circ$ or so to the line of sight (Urry & Padovani 1995). Significant flux variations in the whole range of electromagnetic spectrum on time scale of less than a day to several years are common in blazars. Their radiation at all wavelengths is predominantly non thermal and strongly polarized ($> 3\%$) in radio to optical bands.

Blazar variability can be broadly divided into 3 classes viz. micro variability or intra-night variability or intra-day variability, short term outbursts and long term trends. Variations in flux of a few tenth of a magnitude in a time scale of tens of minutes to a few hours (less than a days) is often known as intra-day variability (IDV) (Wagner & Witzel 1995). Short term outbursts can range from weeks to months and long term trends can have time scales of months to several years.

Study of optical and near-IR variability of blazars on diverse time scales was carried out by several groups (Miller & McGimsey 1978; Xie et al. 1988; Webb et al. 1988; Kidger & de Diego 1990; Carini 1990; Carini et al. 1992; Heidt & Wagner 1996; Bai et al. 1998, 1999; Fan & Lin 1999; Ghosh et al. 2000; Gupta et al. 2002, 2004; Stalin et al. 2005; and references therein). The first convincing evidence of optical IDV was found in BL Lacertae by Miller et al. (1989). The typical optical IDV found in most of the blazars is $\sim 0.01 \text{ mag hr}^{-1}$. Carini (1990) observed a sample of 20 blazars and found most of them showing detectable inter-night variations. He also noted that in observing runs of more

than 8 hours, the probability of detecting significant IDV was $\sim 80\%$. Subsequently, Heidt & Wagner (1996) observed a sample of 34 radio selected BL Lacs and detected IDV in 28 (i.e. 82%) sources out of which 75% sources showed significant variation with in < 6 hours which further supports the finding of high frequency of occurrence of IDV in blazars. In our recent paper (Gupta & Joshi, 2005), we studied the frequency of occurrence of optical IDV in different classes of AGNs and found about 10% (18/174) radio-quiet AGNs, 35–40% (41/115) radio-loud AGNs (excluding blazars) and 70% (79/113) blazars to show IDV (in fact ~ 80 – 85% blazars show IDV, if observed for more than 6 hours).

Mrk 501 is one of the most interesting and nearby BL Lac object at $z = 0.034$ which makes it the second closest known BL Lac object after Mrk 421 ($z = 0.031$). Mrk 501 has been studied for variability in all regions of the electromagnetic spectrum (e.g. Fan & Lin 1999, Kataoka et al. 1999, Sambruna et al. 2000, Ghosh et al. 2000, Xue & Cui 2005, Gliozzi, et al. 2006, and references therein). In optical region this source has been studied by several groups e.g. Stickel et al. (1993) have reported variation of 1.3 magnitude in luminosity; Heidt & Wagner (1996) have reported $\sim 32\%$ variation in flux in less than two weeks time; Ghosh et al. (2000) have made 10 nights observations on Mrk 501 during March to June, 1997 to search for rapid variability and reported rapid variability in 7 nights; and recently, Fan et al. (2004) observed Mrk 501 for two hours in one night in October 2000 and found no significant variation.

The variability in blazars is mainly attributed to either due to the disc instability or the activity in the jet. IDV reported in the flaring and high state is generally attributed to the shock moving down the inhomogeneous medium in the jet. But small amplitude variation in the low state of blazar could be due to instability in the accretion disk (Witta et al. 1991, 1992; Chakrabarti & Wiita 1993; Mangalam & Wiita 1993). Recently, it is noticed that, in the low luminosity AGNs, accretion disk is radiatively inefficient (Chiaberge et al.

2006; Chiaberge & Macchetto 2006; Macchetto & Chiaberge 2007; Capetti et al. 2007). So, there will be an alternative way to explain the IDV in the low-state of blazars, in which a weak jet emission will be responsible for the IDV. So far there is no clear answer to this. There is a need to study IDV and short term variability in the optical bands with a good sampling in time when the source is in low state. In view of this we pursued the present study to address both the IDV and short term variability on Mrk 501.

This paper is structured as follows: section 2 describes photometric observations and data reductions, section 3 present the results, and discussions and conclusions are presented in section 4.

2. Observations and Data Reduction

Observations were made from two places: Mount Abu Observatory of Physical Research Laboratory, India and Sobaeksan Optical Astronomy Observatory, South Korea.

Observations from Mount Abu Observatory:

Photometric monitoring of Mrk 501 was done in B Johnson and R Cousins passbands using a thinned back illuminated Tektronix $1K \times 1K$ CCD detector at f/13 Cassegrain focus of the 1.2 meter telescope at Gurushikhar, Mount Abu, India. To improve the S/N ratio, 2×2 on chip binning was done resulting in pixel size of 0.634 arcsec in both the dimension of the sky. The entire CCD chip covers $\sim 5.4 \times 5.4$ arcmin² of the sky. The readout noise and gain of the CCD chip were 4 electrons and 10 electrons/ADU respectively. Exposure time for B and R passband were 300s and 150s respectively. The average seeing during the observing run remained at 1.5 arcsec. For flat field correction, twilight flats and bias frames were taken every night.

For each night median bias and median flat frames were constructed which were used

in image processing. Image processing (bias subtraction, flat-fielding and cosmic rays removal), photometric reduction (getting instrumental magnitude of stars and Mrk 501) and calibration were done at Physical Research Laboratory, Ahmedabad, India. Image processing was done using standard routines in the IRAF package.

Star no. 1, 4 and 6 (see Villata et al., 1998) in the field of Mrk 501 were selected as comparison stars. But, for the observing run March 8-10, 2006, star no. 1 was saturated in 6 out of 9 R-band image frames and star no. 4 was found to be unstable, so, we used star no. 6 to calibrate the Mrk 501 data obtained in March 2000. Observations taken in April 2000 were calibrated using star no. 1. In April 2000 observations star no. 4 and 6 were having poor S/N ratio compared to Mrk 501. There is advantage, sky variation (seeing) and cloud effects are effectively eliminated by Instrumental magnitude of Mrk 501 and standard stars in the field of Mrk 501 were determined with the help of DAOPHOT II package (Stetson 1987, 1992) using concentric aperture photometric technique taking apertures of radii 5.0, 7.0, 9.5 and 12.0 pixels. The data reduced with different aperture radii were found in good agreement. However, it was noticed that the best signal to noise ratio was obtained with aperture radius of 9.5 pixels (6 arcsec $\sim 4 \times$ FWHM). Stars in different image frames of Mrk 501 field were cross matched by using DAOMATCH routine in DAOPHOT II package.

Observations from Sobaeksan Optical Astronomy Observatory:

Photometric observations of Mrk 501 were also carried out in V and R passbands with the 61 cm Richey-Chretien telescope (f/13.5) and PM512 CCD Camera at the Sobaeksan Optical Astronomy Observatory, South Korea. The field of view of the CCD image is 4.3×4.3 arcmin² and its pixel scale is 0.5 arcsec/pixel. The gain is 9 electrons/ADU, and the readout noise is 10 electrons. The exposure time varies between 150s and 300s. Maximum exposure time is 300s due to unstable tracking of the telescope. The CCD uses an LN2 cooling system. Bias images were taken at the beginning and the end of the observation. Sky flat images were taken at both dusk and dawn. The instrumental magnitudes were

obtained using the aperture photometry routine in IRAF/DAOPHOT package as discussed above. For aperture photometry, aperture radii were decided depending on the seeing, that is, 3 or 4 times of the FWHM. In the image frames 3 comparison (standard) stars, no. 1, 4 and 6 were present. Data are calibrated using star no. 1. We did not use star no. 4 and 6 for calibration, since these stars were having poor S/N ratio compared to Mrk 501.

Observation log and the intra-day variability results are listed in Table 1. Photometric data in B, V and R passbands are given in Table 2, 3 and 4 respectively. Photometric software DAOPHOT does not give the actual internal error of brightness but it gives the photon noise. The internal photometric errors of brightness for each passband are estimated using artificial addstar experiment as described by Stetson (1987). We found the standard deviation (σ) = 0.015, 0.012 and 0.010 for B, V and R passbands respectively.

3. Results

3.1. Flux and Color Variations

3.1.1. Intraday Variability

Light curves of comparison star (instrumental mag.), Mrk 501 (instrumental mag.) and Mrk 501 (standard mag.) in V and R passbands are plotted in Fig. 1 and Fig. 2. For plotting purpose, only the data for those nights are taken where the data points are more than seven. We report here objectively the presence or absence of IDV at a confidence level of more than 5σ .

B Passband: The source has been observed in B passband on 3 nights but there are only a few data points (three) in each night and hence the data are not plotted. Measurements in B passband show variation to the extent of 0.013 mag on March 8, 0.080

mag on March 9 and 0.015 mag on March 10. Looking at the data of March 9, we notice fluctuations in brightness of comparison star, which might be partly responsible for the apparent variation of 0.015 mag seen in Mrk 501, so the variation detected is doubtful. Hence as per our criterion, there is no significant IDV seen in B band data.

V Passband: Light curves in V passband show variation to the extent of 0.079 mag on March 30 (Fig. 1 (a)). Visual inspection of the figure indicates that the the variation seen in Mrk 501 might be due to the fluctuations in comparison star. So, the variation seen may not be a genuine IDV. Variations are also noticed on other nights: 0.019 mag on March 31, 0.026 mag on May 1, 0.035 mag on May 2 and 0.034 mag on May 3. However, as per our IDV detection criterion, we conclude no detection of significant IDV during the observing run of 5 nights.

R Passband: Light curves in R passbands show variation to the extent of 0.004 mag on March 8, 0.027 mag on March 9, 0.009 mag on March 10, 0.022 mag on March 30, 0.029 mag on March 31, 0.147 mag on April 1, 0.053 mag on April 5, 0.018 mag on April 6, 0.021 mag on May 1, 0.077 mag on May 2 and 0.039 mag on May 3. The data on April 1 are noisy, therefore the variation of 0.147 mag seen in this night is not taken as genuine IDV. Visual inspection of light curve on May 2 shows fluctuations in the magnitude of comparison star and hence the apparent variation seen in Mrk 501 might be partly due to this. Therefore, the variation seen is not considered as real. So, out of 11 nights observations in R passband, IDV is seen only in 1 night, i.e April 5.

Variations, similar to that seen in the present work, have also been noted earlier by other researchers e.g. on one occasion Ghosh et al. (2000) have reported variation of 0.13 mag in V band in less than 30 min while on the other occasion they report brightness variation of 0.04 mag in 29 minutes followed by steady brightness. According to Ghosh et al. (2000), the source was not in active phase during their observing run. Fan et al. (2004)

have reported the results on Mrk 501 based on the continuous observing run of two hours in October 2000 in R band and no significant variations were noticed. A blazar generally show IDV of relatively large amplitude during its outburst period while it shows very small flux variation or no obvious variation during the quiescent state. Thus during our observing run, Mrk 501 appears to be in quiescent state as the intraday brightness variations detected are less than 6 to 7%.

3.1.2. Short Term Variability

In Fig. 4 we have plotted all the data points in B, V and R passbands against the time in JD. The inter-night brightness variations are distinctly visible in the figure; the maximum variation of the source in V passband being 0.19 mag (between its faintest level at 13.78 mag on JD 2451635.320 and the brightest level at 13.59 mag on JD 2451667.237) whereas in R passband it has varied by 0.29 mag (between its faintest level at 13.46 mag on JD 2451613.505 and the brightest level at 13.17 mag on JD 2451667.194). Data of April 1 being noisy, are not included in the short term variability analysis. During the observing run of about 8 weeks, the source shows brightness variation of about $\sim 15\%$ in V passband and $\sim 25\%$ in R passband. Heidt & Wagner (1996) have reported $\sim 32\%$ variation in flux in less than two weeks time which is larger than the variation seen in the present work (the maximum brightness variation detected in the present work is about 25% in about 2 months time).

3.1.3. Color Variation

In Fig. 4 panel (d) and (e), nightly average color ($B_{ave} - R_{ave}$) and ($V_{ave} - R_{ave}$) respectively are plotted against the time (in JD). For plotting purpose instead of taking

the mean time (in JD) of the observing run, we have taken JD at 00h 00m 00s UT of that specific date. In Fig. 2, panel (d), there is no significant change in $(B_{ave} - R_{ave})$ color but in panel (e) the variation in color $(V_{ave} - R_{ave})$ is apparent. The effect of variation in V and R magnitude (see panel (c) and (d)) has reflected in the $(V_{ave} - R_{ave})$ color showing, the source has become 0.19 mag bluer during the observing campaign (between 0.53 at JD 2451635.50 and 0.33 at JD 2451669.50).

3.2. Variability time scale

Fig. 2, panel (g) shows the light curve of Mrk 501 in R-band on April 5, 2000. During the period JD 2451640.412 to JD 2451640.421, the luminosity has decreased by 0.04 mag and then a rapid flare has occurred at epoch JD 2451640.421, reaching a brightness excursion of 0.05 mag at JD 2451640.431. Just after the flare, again there is a decrease in luminosity of 0.02 mag between JD 2451640.431 and JD 2451640.438. There after the source became steady (see Fig 2 (g) top panel).

To search for the time scale of variation quantitatively, we carried out Structure Function (SF) analysis on the R-band IDV of Fig. 2 (g) (top panel). SF is usually calculated twice by using an interpolation algorithm, first starting from the beginning of the time series and proceeding forward and then starting from the end and proceeding backward. This will give two slightly different SF curves but will provide a rough assessment of the errors due to the interpolation process (Wu et al. 2006).

The first order structure function is equivalent to the power spectrum density (PSD) and is a powerful tool to search for periodicities and time scales in a time series data (see e.g. Rutman 1978; Simonetti, Cordes & Heeschen 1985; Paltani et al. 1997). The first order

SF for a light curve having uniformly spaced data points is defined as

$$D_a^1(k) = \frac{1}{N_a^1(k)} \sum_{i=1}^N w(i)w(i+k)[a(i+k) - a(i)]^2 \quad (1)$$

where k is time lag, $N_a^1(k) = \sum w(i)w(i+k)$ and the weighting factor $w(i)$ is 1 if a measurement exists for the i th interval, 0 otherwise. The squared uncertainties in the estimated SF is

$$\sigma^2(k) = \frac{8\sigma_{\delta f}^2}{N^1(k)} D_f^1(k) \quad (2)$$

where $\sigma_{\delta f}^2$ is the measured noise variance.

Since the data sampling in our light curve is quasi-uniform, we used interpolation method to determine the first order SF. For any time lag k , the value of $a(i+k)$ was calculated by linear interpolation between the two adjacent data points. In a similar fashion SF was calculated for a large number of IDV light curves (Sagar et al. 2004, Stalin et al. 2005). The behavior of the first order SF have the following types:

(i) If the source first order SF does not display any plateau, it represents the time scale of the variability to be larger than the length of the data.

(ii) If the source first order SF display a plateau followed by a dip in the SF, the dip indicates a possible cycle and plateau the time scale of the variability.

Fig. 3 displays the SF of the light curve of top panel of Fig 2. (g). SF display one plateau followed by a dip. From the plateau we deduce the variability time scales to be 0.01 day i.e ~ 15 min.

4. Discussions & Conclusions

From our observations on Mrk 501 during March - May, 2000, we find the existence of IDV (to the extent of $\sim 6-7$ %) in R band on one occasion. The source has shown short

term flux variability and total variation detected in our observations in V passband is $\sim 15\%$ and in R passband is $\sim 25\%$. The data do not show any significant variation in (B–R) color but (V–R) color has varied by about 0.2 mag. Though we see some variation in brightness in the light curves, it appears that Mrk 501 was not in active phase during our observations.

We have detected variation, on April 5, in time scale of ~ 15 min in Mrk 501. Our observations do not show any periodicity or quasi-periodicity in intra-day or short time scales. But, in some other blazars quasi periodic variations have been reported earlier on longer as well as shorter time scales e.g. quasi periodic variations, existing simultaneously in optical and radio wavelength, are reported on the timescale of 1 to 7 days in S5 0716+714 (Quirrenbach et al. 1991). The same source on other occasion shows quasi periodic variation in time scale of 4 days in optical region (Heidt & Wagner 1996). Quasi periodic variations were also found in the PKS 2155-304 in UV and X-ray wavelength (Urry et al. 1993). On short time scale, for example, periodic flux variation is reported in OJ 287 in radio as well as in optical band. Valtaoja et al. (1985) have reported 15.7 min periodicity at 37 GHz, Carrasco et al. (1985) have reported 23 minute period in their observations in optical B passband and Carini et al. (1992) have shown the optical periodicity of 32 min.

Several models have been developed to explain the IDV and short term variability in blazars viz. the shock-in-jet models, accretion-disk based models (e.g. Wagner & Witzel 1995; Urry & Padovani 1995; Ulrich, Maraschi & Urry 1997 and references therein). The detection of quasi-periodicity in time scale of minutes to less than a week in some of the blazars could be taken as evidence for the existence of accretion disk pulsation, or the presence of a single dominating hot-spot on the accretion disk, or of a helical structure in a jet (Vila 1979, Mangalam & Wiita 1993, Chakrabarti & Wiita 1993). Quasi-periodic variation may also be attributed to a precessing jet. So search for periodic variations has

great interests. The variability reported in the present work could be explained by any of the above models.

However, the variability detected in the low state of blazars can be explained on the basis of some kind of instability in the accretion disk, because in the low state, jet emission is less dominant over the thermal emission from the disk. Within unified schemes, the blazars are seen nearly face on, hence any accretion disk fluctuations should be directly visible. The models for the flares randomly emerging at different locations and at different time on accretion disks could be very relevant to the variations seen in blazars at low-state. Eclipse of the hot spot by parts of the disk between the individual spot and the observer could be the other possible mechanism to produce variability in blazars at low-state. There often exists a range of azimuthal positions at a given radius within which the spot is eclipsed, and this is directly depends on the geometry of disk and the viewing angle of observer. The central black hole mass is expected to shed some light on the evolution process in AGNs (Barth et al. 2002, Fan 2003). There are several ways to find the BH mass but there is no consensus on this and the BH mass reported in the literature for a particular source differ significantly. The BH mass for Mrk 501, estimated by many authors, is in the range $(0.01 - 3.4) \times 10^9 M_{\odot}$ (Barth et al. 2002, Fan et al. 1999, Merritt & Ferrarese 2001, Rieger & Mannheim 2003). For Mrk 501, our optical observation show the variability time scale of 15 min. We assume that detected IDV is due to an instability in the vicinity of the super massive BH and the size of emitting region is taken as $R = ct$, where t is the variability time scale (i.e 15min). Further assuming that the 15 min variability time scale corresponds to instability or disk pulsation on the accretion disk at a distance of $R = 5 R_S$ where $R_S = 2GM/c^2$ is Schwarzschild radius, the mass of the super massive BH, M can be estimated by using the formula: $M = c^3t/10G = 1.20 \times 10^8 M_{\odot}$. The Eddington luminosity for a black hole of mass M is given by $L_E = 1.3 \times 10^{38} (M/M_{\odot}) \text{ erg s}^{-1}$ (Witta 1985), which in the present case will be $L_E = 1.56 \times 10^{46} \text{ erg s}^{-1}$. The result is in the range of $(0.01 -$

$3.4) \times 10^9 M_{\odot}$, and hence consistent with other results.

There is an alternative way to explain the IDV detected in the present work. In the recent work (e.g. Chiaberge et al. 1999, 2006; Chiaberge & Macchetto 2007; Capetti et al. 2007; Macchetto & Chiaberge 2007 and references therein), by analyzing R band HST images of a sample of 33 FR I sources, they were able to detect the unresolved optical nuclear sources. They found that optical and radio nuclear luminosities were strongly correlated. They also found tight correlation between the radio and X-ray luminosities measured from Chandra observations (Balmaverde et al. 2006). Furthermore, the correlation between radio, optical and X-ray emission extends to the large population of radio-loud AGNs found in early-type galaxies, with luminosities smaller by a factor ~ 1000 with respect to classical low-luminosity radio-galaxies (Balmaverde & Capetti 2006). According to these findings the nuclear emission in low luminosity radio-loud AGNs is dominated by non-thermal emission from the base of the jet. Assuming FR I and BL Lacs unification, which is yet to be established, the alternate possibility is that the IDV seen in BL Lacs could arise in the jet. Considering this model, the detected small IDV in the low-state of the BL Lac object Mrk 501 might be due to a weak emission from the base of the jet.

It will be really interesting to start a long term multi-color optical monitoring program of BL Lac objects in their low-states to search for the IDV. We believe, with focused effort, we can make a large data set, and we may be able to find which model is more appropriate to discuss the results of IDV in the low-state of BL Lac objects. At this stage, we leave it as an open problem.

We thank the anonymous referees for their useful suggestions. A. C. Gupta, W. G. Deng and J. M. Bai gratefully acknowledge the financial support from the National Natural Science Foundation of China (grant nos. 10533050 and 10573030). The research work at Physical Research Laboratory was funded by the Department of Space, Government of

India. M. G. Lee acknowledges the financial support from the BK21 Project of the Korean government. IRAF is distributed by NOAO, USA.

REFERENCES

- Antonucci, R. 1993, *ARA&A*, 31, 473
- Bai, J. M., Xie, G. Z., Li, K. H., et al. 1998, *A&AS*, 132, 83
- Bai, J. M., Xie, G. Z., Li, K. H., et al. 1999, *A&AS*, 136, 455
- Balmaverde, B. & Capetti, A. 2006, *A&A*, 447, 97
- Balmaverde, B. & Capetti, A. & Grandi, P. 2006, *A&A*, 451, 35
- Barth, A. J., Ho, L. C., Sargent, W. L. W. 2002, *ApJ*, 566, L13
- Browne, I. W. A. 1983, *MNRAS*, 204, 23
- Capetti, A., Axon, D. J., Chiaberge, M., et al. 2007, *A&A*, 471, 137
- Carini, M. T. 1990, Ph.D. dissertation, Georgia State University, USA
- Carini, M. T., Miller, H. R., Nobel, J. C., & Goodrich, B. D. 1992, *AJ*, 104, 15
- Carrasco, L., Dultzin-Hacyan, D., & Cruz-Gonzalez. 1985, *Nature*, 314, 146
- Chakrabarti, S. K., & Wiita, P. J. 1993, *ApJ*, 411, 602
- Chiaberge, M., Capetti, A. & Celotti, A. 1999, *A&A*, 349, 77
- Chiaberge, M., Gilli, R., Macchetto, F. D. et al. 2006, *ApJ*, 651, 728
- Chiaberge, M. & Macchetto, D. 2007, *AAS*, 209, 7217
- Fan, J. H. 2003, *ApJ*, 585, L23
- Fan, J. H., Kurtanidze, O. M., Nikolashvili, M. G., et al. 2004, *ChJAA*, 4, 133
- Fan, J. H., & Lin, R. G. 1999, *ApJS*, 121, 131

- Fan, J. H., Xie, G. Z., & Bacon, R. 1999, *A&AS*, 136, 13
- Ghosh, K. K., Ramsey, B. D., Sadun, A. C., et al. 2000, *ApJS*, 127, 11
- Giozzi, M., Sambruna, R. M., Jung, I., et al. 2006, *ApJ*, 646, 61
- Gupta, A. C., Banerjee, D. P. K., Ashok, N. M., & Joshi, U. C. 2004, *A&A*, 422, 505
- Gupta, A. C., & Joshi, U. C. 2005, *A&A*, 440, 855
- Gupta, A. C., Joshi, U. C., & Fan, J. H. 2002, *Ap&SS*, 282, 655
- Heidt, J., & Wagner, S. J. 1996, *A&A*, 305, 42
- Kataoka, J., Mattox, J. R., Quinn, J. et al. 1999, *ApJ*, 514, 138
- Kidger, M. R., & de Diego, J. A. 1990, *A&A*, 227, L25
- Macchetto, F. D. & Chiaberge, M. 2007, *IAUS*, 238, 273
- Mangalam, A. V., & Wiita, P. J. 1993, *ApJ*, 406, 420
- Merritt, D., & Ferrarese, L. (2001) in *The Central Kiloparsec of Starbursts and AGNs*,
edited by J. H. Knapen, J. E. Beckman, et al. *ASP Conf. Proc.* 249, p335
- Miller, H. R., Carini, M. T., & Goodrich, B. D. 1989, *Nature*, 337, 627
- Miller, H. R., & McGimsey, B. Q. 1978, *ApJ*, 220, 19
- Paltani, S., Courvoisier, T. J.-L., Blecha, A., & Bratschi, P. 1997, *A&A*, 327, 539
- Quirrenbach, A., Witzel, A., Wagner, S. J., et al. 1991, *ApJ*, 372, L71
- Rieger, F. M., & Mannheim, K. 2003, *A&A*, 397, 121
- Rutman, J. 1978, *Proc. IEEE*, 66, 1048

- Sagar, R., Stalin, C. S., et al. 2004, MNRAS, 348, 176
- Sambruna, R. M., Aharonian, F. A., & Krawczynski, H. 2000, ApJ, 538, 127
- Simonetti, J. H., Cordes, J. M., & Heeschen, D. S. 1985, ApJ, 296, 46
- Stalin, C. S., Gupta, A. C., et al. 2005, MNRAS, 356, 607
- Stickel, M., Fried, J. W., & Kühn, H. 1993, A&AS, 98, 393
- Stetson, P. B., 1987, PASP, 99, 191
- Stetson, P. B., 1992, IAU col. 136 on stellar photometry – current techniques and future developments, eds. C. J. Butler and I. Elliot, p. 291
- Ulrich, M.-H., Maraschi, L., & Urry, C. M. 1997, ARA&A, 35, 445
- Urry, C. M., Maraschi, L., Edelson, R., et al. 1993, ApJ, 411, 614
- Urry, C. M., & Padovani, P. 1995, PASP, 107, 803
- Valtaoja, E., Lehto, H., Teerikorpi, P., et al. 1985, Nature, 314, 148
- Vila, S. C. 1979, ApJ, 234, 636
- Villata, M., Raiteri, C. M., Lanteri, L., et al. 1998, A&AS, 130, 305
- Wagner, S. J., & Witzel, A. 1995, ARA&A, 33, 163
- Webb, J. R., Smith, A. G., Leacock, R. J., et al. 1988, AJ, 95, 374
- Wiita, P. J. 1985, Physics Report, 123, 117
- Wiita, P. J., Miller, H. R., Carini, M. T., & Rosen, A. 1991, in Structure and Emission Properties of Accretion Disks, ed. J. P. Lasota et al. (Editions Frontieres, Gif-sur-Yvette), IAU Colloq., 129, 557

Wiita, P. J., Mangalam, A. V., & Chakrabarti, S. K. 1992, in AIP Conference Proceedings,
Vol. 254, p. 251

Wu, J., Zhou, X., Wu, Xue-Bing., et al. 2006, AJ, 132, 1256

Xie, G-Z, Lu, R-W, Zhou, Y., et al. 1988, A&AS, 72, 163

Xue, Y., & Cui, W. 2005, ApJ, 622, 160

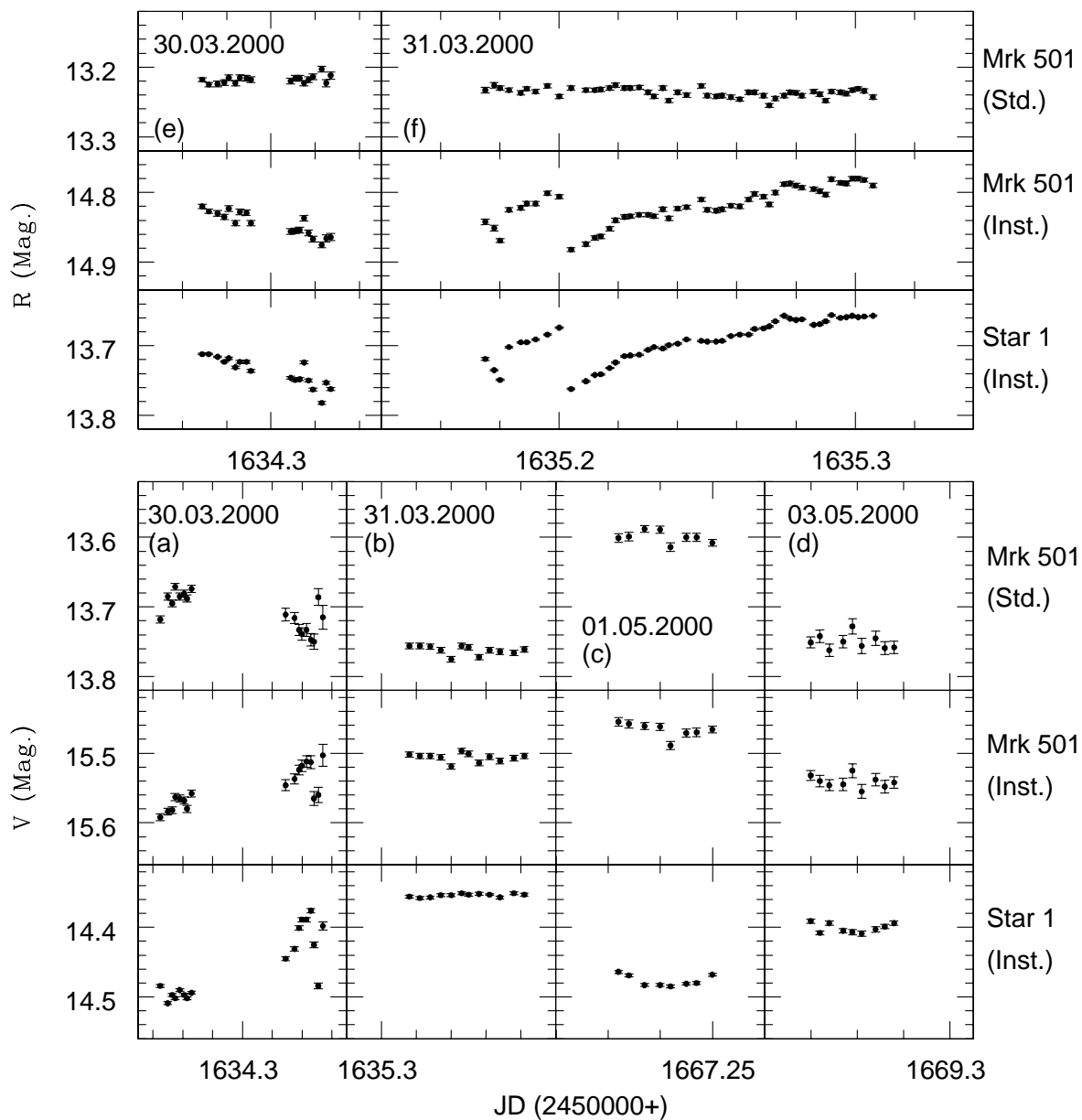


Fig. 1.— Light-curves for V-band are plotted in panel (a), (b), (c) and (d) respectively for March 30, March 31, May 1 and May 3. The R-band light-curves for March 30 and March 31 are plotted respectively in panel (e) and (f).

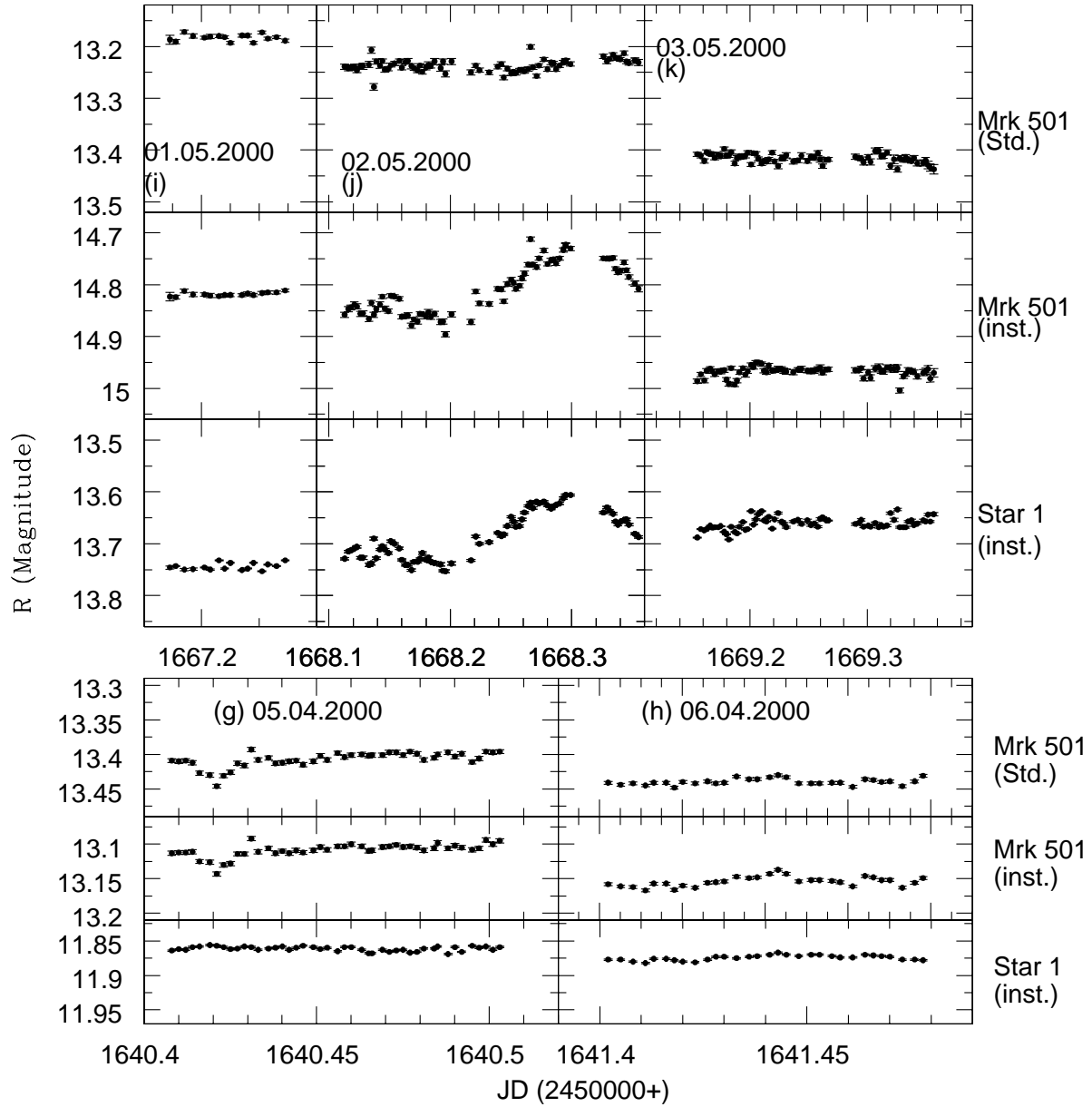


Fig. 2.— The R-band light-curves for April 5, April 6, May 1, May 2 and May 3 are plotted respectively in panel (g), (h), (i), (j) and (k).

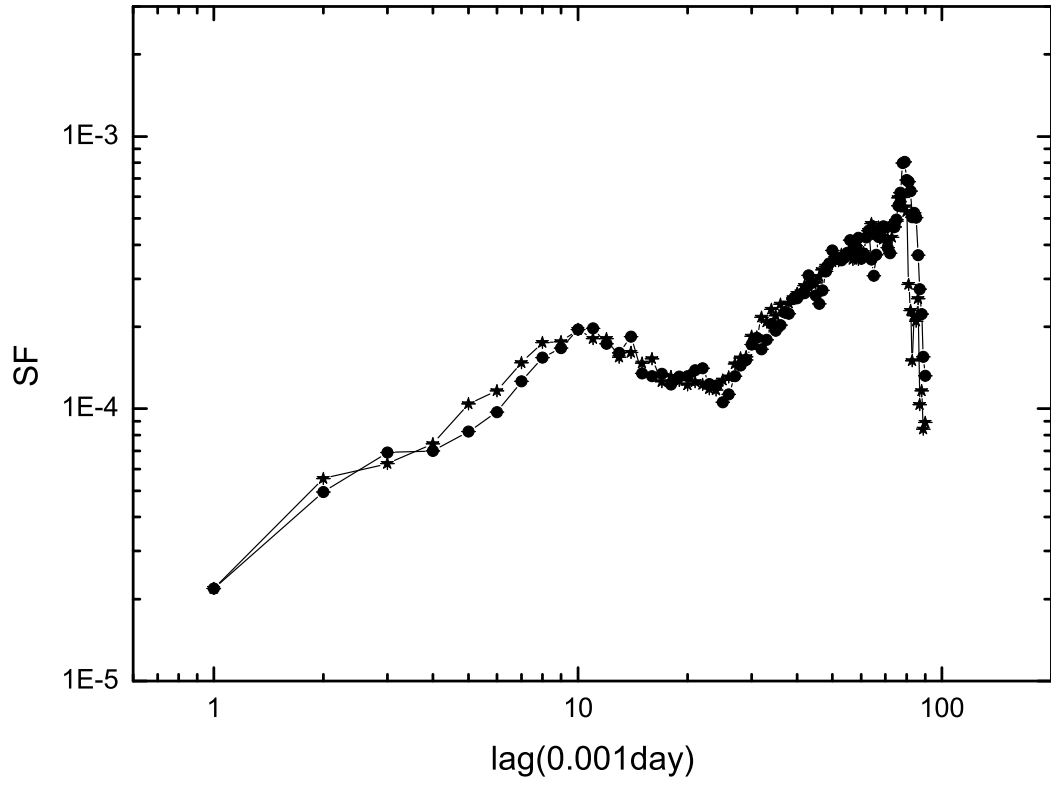


Fig. 3.— First order structure function of the BL Lac object Mrk 501 of the top panel of Fig. 2 (g). Error bars are also plotted in the figure but the size of error bars are less than the size of the symbol, so, not visible clearly.

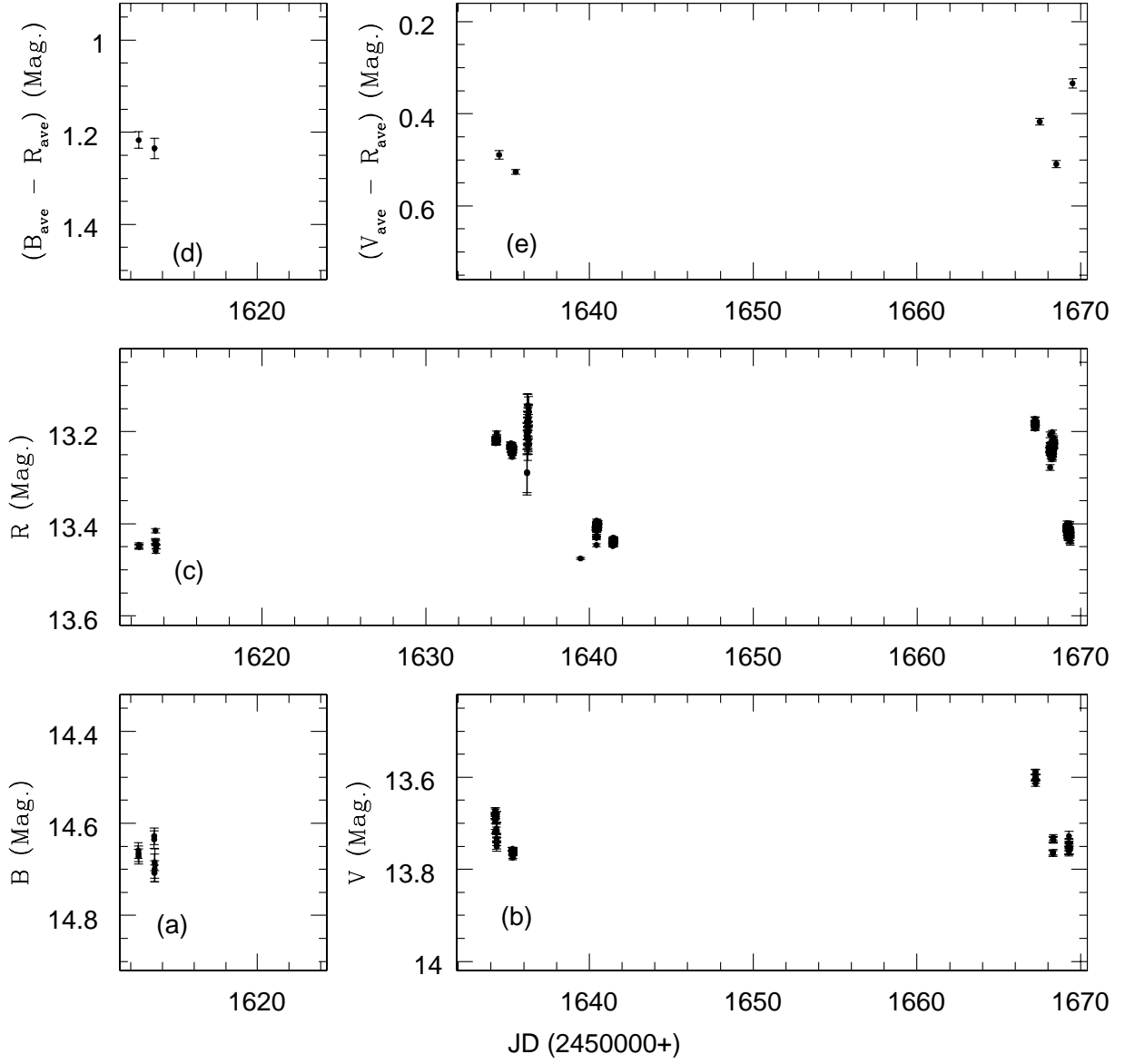


Fig. 4.— Panels a, b, c, d and e represent light-curves in magnitude B,V, R and color ($B_{ave} - R_{ave}$ and $(V_{ave} - R_{ave})$) respectively for the observing run March 8 - May 3, 2000.

Table 1: The complete log of observations of Mrk 501 and IDV status. V and NV represent intraday variability observed and not observed respectively.

Date (dd.mm.yyyy)	Filter	No. of data points	Telescope	IDV Status	Time Scale
08.03.2000	B	3	India	NV	15 min
	R	3	India	NV	
09.03.2000	B	3	India	NV	
	R	4	India	NV	
10.03.2000	B	3	India	NV	
	R	2	India	NV	
30.03.2000	V	17	Korea	NV	
	R	18	Korea	NV	
31.03.2000	V	12	Korea	NV	
	R	49	Korea	NV	
01.04.2000	R	32	Korea	Noisy	
04.04.2000	R	1	India	NV	
05.04.2000	R	45	India	V	
06.04.2000	R	32	India	NV	
01.05.2000	V	8	Korea	NV	
	R	16	Korea	NV	
02.05.2000	V	6	Korea	NV	
	R	76	Korea	NV	
03.05.2000	V	9	Korea	NV	
	R	70	Korea	NV	

Table 2: The B-band data of Mrk 501.

JD (2450000+)	Magnitude	Error
1612.479	14.659	0.017
1612.486	14.666	0.017
1612.493	14.672	0.016
1613.478	14.635	0.019
1613.487	14.628	0.018
1613.494	14.708	0.018
1613.501	14.685	0.018
1613.516	14.700	0.019
1613.525	14.691	0.036

Table 3: The V-band data of Mrk 501.

JD (2450000+)	Magnitude	Error	JD (2450000+)	Magnitude	Error
1634.245	13.718	0.005	1635.334	13.764	0.004
1634.250	13.685	0.005	1635.338	13.766	0.004
1634.253	13.695	0.005	1635.341	13.761	0.004
1634.255	13.671	0.005	1667.232	13.601	0.006
1634.258	13.685	0.005	1667.234	13.599	0.006
1634.261	13.681	0.005	1667.237	13.588	0.005
1634.263	13.688	0.005	1667.240	13.589	0.005
1634.266	13.674	0.005	1667.242	13.614	0.006
1634.329	13.711	0.009	1667.245	13.600	0.006
1634.335	13.716	0.008	1667.247	13.600	0.006
1634.338	13.733	0.008	1667.250	13.608	0.005
1634.340	13.739	0.009	1668.303	13.763	0.006
1634.343	13.733	0.009	1668.307	13.766	0.006
1634.346	13.747	0.009	1668.309	13.735	0.006
1634.348	13.750	0.011	1668.317	13.731	0.006
1634.351	13.686	0.012	1668.321	13.735	0.006
1634.354	13.715	0.017	1668.323	13.737	0.006
1635.308	13.756	0.004	1669.270	13.751	0.008
1635.311	13.756	0.004	1669.272	13.742	0.009
1635.314	13.757	0.004	1669.274	13.762	0.009
1635.317	13.762	0.004	1669.277	13.750	0.009
1635.320	13.775	0.004	1669.279	13.728	0.011
1635.323	13.756	0.004	1669.281	13.756	0.011
1635.325	13.758	0.004	1669.284	13.745	0.010
1635.328	13.772	0.004	1669.286	13.759	0.009
1635.331	13.762	0.004	1669.288	13.758	0.009

Table 4: The R-band data of Mrk 501.

JD (2450000+)	Magnitude	Error	JD (2450000+)	Magnitude	Error	JD (2450000+)	Magnitude	Error
1612.474	13.446	0.005	1635.217	13.230	0.003	1636.184	13.290	0.042
1612.483	13.450	0.005	1635.219	13.226	0.003	1636.186	13.215	0.035
1612.490	13.450	0.005	1635.222	13.230	0.003	1636.203	13.212	0.016
1613.475	13.437	0.005	1635.224	13.230	0.003	1636.206	13.199	0.010
1613.483	13.415	0.005	1635.227	13.229	0.003	1636.208	13.180	0.010
1613.491	13.442	0.005	1635.230	13.236	0.003	1636.211	13.176	0.013
1613.498	13.439	0.005	1635.232	13.242	0.003	1636.214	13.203	0.014
1613.505	13.459	0.005	1635.235	13.230	0.003	1636.216	13.199	0.029
1613.516	13.450	0.005	1635.237	13.248	0.003	1636.218	13.177	0.022
1634.269	13.218	0.003	1635.240	13.236	0.003	1636.220	13.176	0.019
1634.272	13.225	0.003	1635.243	13.240	0.003	1636.222	13.214	0.018
1634.276	13.224	0.004	1635.248	13.227	0.003	1636.224	13.190	0.033
1634.279	13.222	0.004	1635.250	13.241	0.003	1636.226	13.232	0.030
1634.281	13.215	0.004	1635.253	13.242	0.003	1636.228	13.189	0.040
1634.284	13.223	0.004	1635.255	13.241	0.003	1636.240	13.143	0.025
1634.286	13.215	0.004	1635.258	13.243	0.003	1636.242	13.214	0.023
1634.289	13.216	0.004	1635.261	13.246	0.003	1636.245	13.165	0.025
1634.291	13.218	0.004	1635.264	13.236	0.003	1636.248	13.172	0.026
1634.309	13.220	0.004	1635.266	13.236	0.003	1636.250	13.212	0.032
1634.311	13.216	0.004	1635.269	13.241	0.003	1636.252	13.179	0.036
1634.313	13.216	0.004	1635.271	13.255	0.003	1636.254	13.202	0.024
1634.315	13.223	0.004	1635.273	13.245	0.003	1636.256	13.219	0.022
1634.317	13.218	0.004	1635.276	13.241	0.003	1636.258	13.160	0.018
1634.319	13.214	0.004	1635.278	13.236	0.003	1636.260	13.198	0.013
1634.323	13.203	0.004	1635.280	13.237	0.003	1636.262	13.175	0.012
1634.325	13.223	0.005	1635.282	13.241	0.003	1636.278	13.151	0.027
1634.327	13.212	0.005	1635.286	13.235	0.003	1636.282	13.179	0.037
1635.175	13.233	0.004	1635.288	13.239	0.003	1636.284	13.218	0.031
1635.178	13.226	0.004	1635.290	13.248	0.003	1639.445	13.475	0.002
1635.180	13.230	0.003	1635.292	13.235	0.003	1640.408	13.409	0.003
1635.183	13.233	0.003	1635.295	13.236	0.003	1640.410	13.410	0.003
1635.187	13.237	0.003	1635.297	13.238	0.003	1640.412	13.409	0.003
1635.189	13.231	0.003	1635.299	13.233	0.003	1640.414	13.412	0.003
1635.192	13.235	0.003	1635.301	13.231	0.003	1640.416	13.427	0.003
1635.196	13.227	0.003	1635.303	13.234	0.003	1640.419	13.430	0.003
1635.200	13.242	0.003	1635.306	13.243	0.003	1640.421	13.446	0.003
1635.204	13.230	0.003	1636.176	13.207	0.010	1640.423	13.431	0.003
1635.209	13.233	0.003	1636.178	13.204	0.022	1640.425	13.426	0.003
1635.212	13.233	0.003	1636.180	13.288	0.049	1640.427	13.413	0.003
1635.214	13.232	0.003	1636.182	13.178	0.060	1640.429	13.416	0.003

JD (2450000+)	Magnitude	Error	JD (2450000+)	Magnitude	Error	JD (2450000+)	Magnitude	Error
1640.431	13.393	0.003	1641.418	13.448	0.002	1667.229	13.189	0.003
1640.433	13.408	0.003	1641.420	13.440	0.002	1668.113	13.239	0.005
1640.436	13.405	0.003	1641.423	13.442	0.002	1668.116	13.242	0.005
1640.438	13.413	0.003	1641.426	13.439	0.002	1668.118	13.241	0.005
1640.440	13.412	0.003	1641.428	13.442	0.002	1668.121	13.239	0.005
1640.442	13.410	0.003	1641.430	13.441	0.002	1668.123	13.246	0.005
1640.444	13.409	0.003	1641.433	13.432	0.002	1668.126	13.239	0.005
1640.446	13.415	0.003	1641.436	13.436	0.002	1668.128	13.238	0.006
1640.449	13.410	0.003	1641.438	13.436	0.002	1668.133	13.235	0.006
1640.451	13.402	0.003	1641.441	13.433	0.002	1668.135	13.207	0.006
1640.453	13.408	0.003	1641.443	13.430	0.002	1668.137	13.278	0.006
1640.456	13.398	0.003	1641.445	13.433	0.002	1668.139	13.229	0.005
1640.458	13.404	0.003	1641.448	13.442	0.002	1668.142	13.237	0.005
1640.460	13.401	0.003	1641.451	13.442	0.002	1668.144	13.228	0.004
1640.463	13.400	0.003	1641.453	13.442	0.002	1668.146	13.245	0.005
1640.465	13.402	0.003	1641.456	13.441	0.002	1668.149	13.243	0.004
1640.466	13.401	0.003	1641.458	13.441	0.002	1668.151	13.236	0.004
1640.469	13.401	0.003	1641.461	13.447	0.002	1668.154	13.233	0.004
1640.471	13.397	0.003	1641.464	13.436	0.002	1668.158	13.228	0.004
1640.473	13.397	0.003	1641.466	13.437	0.002	1668.160	13.241	0.004
1640.475	13.401	0.003	1641.468	13.440	0.002	1668.163	13.230	0.004
1640.477	13.396	0.003	1641.470	13.439	0.002	1668.165	13.228	0.005
1640.479	13.399	0.003	1641.473	13.446	0.002	1668.168	13.238	0.005
1640.481	13.408	0.003	1641.476	13.439	0.002	1668.170	13.242	0.004
1640.484	13.405	0.003	1641.478	13.431	0.002	1668.173	13.246	0.005
1640.485	13.400	0.003	1667.189	13.187	0.009	1668.175	13.237	0.004
1640.488	13.397	0.003	1667.191	13.191	0.004	1668.177	13.249	0.004
1640.490	13.403	0.003	1667.194	13.172	0.004	1668.180	13.240	0.005
1640.492	13.399	0.003	1667.197	13.180	0.004	1668.182	13.236	0.006
1640.495	13.411	0.003	1667.201	13.183	0.003	1668.184	13.237	0.005
1640.497	13.406	0.003	1667.203	13.181	0.004	1668.187	13.229	0.006
1640.499	13.396	0.003	1667.206	13.180	0.003	1668.192	13.242	0.006
1640.501	13.397	0.003	1667.208	13.182	0.003	1668.194	13.229	0.005
1640.503	13.396	0.003	1667.210	13.193	0.003	1668.196	13.253	0.006
1641.402	13.441	0.002	1667.214	13.179	0.003	1668.201	13.229	0.006
1641.405	13.444	0.002	1667.216	13.179	0.003	1668.217	13.250	0.005
1641.408	13.442	0.002	1667.218	13.193	0.003	1668.221	13.237	0.004
1641.411	13.445	0.002	1667.221	13.173	0.003	1668.224	13.246	0.004
1641.413	13.441	0.002	1667.223	13.185	0.003	1668.232	13.250	0.004
1641.416	13.441	0.002	1667.226	13.182	0.003	1668.239	13.239	0.004

JD (2450000+)	Magnitude	Error	JD (2450000+)	Magnitude	Error	JD (2450000+)	Magnitude	Error
1668.242	13.234	0.004	1669.155	13.408	0.004	1669.244	13.411	0.006
1668.244	13.260	0.004	1669.158	13.411	0.004	1669.249	13.421	0.004
1668.247	13.243	0.004	1669.161	13.421	0.004	1669.252	13.413	0.005
1668.250	13.252	0.004	1669.163	13.404	0.004	1669.255	13.415	0.005
1668.252	13.249	0.004	1669.166	13.407	0.004	1669.258	13.406	0.005
1668.254	13.251	0.004	1669.168	13.408	0.004	1669.260	13.418	0.005
1668.257	13.246	0.004	1669.170	13.415	0.004	1669.262	13.431	0.004
1668.259	13.245	0.004	1669.173	13.409	0.004	1669.265	13.419	0.004
1668.261	13.248	0.004	1669.175	13.412	0.004	1669.267	13.418	0.004
1668.264	13.244	0.004	1669.178	13.398	0.004	1669.290	13.413	0.005
1668.266	13.201	0.004	1669.180	13.411	0.004	1669.293	13.415	0.004
1668.268	13.240	0.004	1669.182	13.410	0.004	1669.295	13.417	0.004
1668.271	13.257	0.004	1669.184	13.404	0.004	1669.297	13.424	0.005
1668.273	13.237	0.004	1669.187	13.426	0.004	1669.301	13.414	0.005
1668.277	13.225	0.004	1669.189	13.415	0.004	1669.303	13.423	0.006
1668.280	13.244	0.004	1669.191	13.412	0.004	1669.307	13.402	0.006
1668.285	13.233	0.004	1669.194	13.413	0.004	1669.310	13.401	0.006
1668.283	13.231	0.004	1669.196	13.411	0.004	1669.312	13.412	0.005
1668.287	13.244	0.004	1669.198	13.405	0.004	1669.314	13.411	0.005
1668.290	13.237	0.004	1669.201	13.428	0.004	1669.317	13.405	0.005
1668.293	13.231	0.004	1669.203	13.406	0.004	1669.320	13.431	0.006
1668.295	13.229	0.004	1669.205	13.407	0.004	1669.323	13.418	0.008
1668.297	13.227	0.004	1669.207	13.417	0.004	1669.326	13.437	0.006
1668.299	13.234	0.004	1669.210	13.426	0.004	1669.328	13.416	0.005
1668.326	13.219	0.004	1669.212	13.421	0.004	1669.331	13.419	0.004
1668.329	13.229	0.004	1669.214	13.422	0.004	1669.333	13.414	0.005
1668.331	13.224	0.004	1669.216	13.418	0.004	1669.335	13.418	0.005
1668.334	13.216	0.004	1669.219	13.405	0.004	1669.338	13.421	0.004
1668.336	13.222	0.004	1669.221	13.422	0.004	1669.340	13.415	0.004
1668.338	13.223	0.004	1669.224	13.431	0.005	1669.343	13.426	0.005
1668.340	13.225	0.004	1669.227	13.416	0.005	1669.348	13.425	0.006
1668.343	13.213	0.004	1669.229	13.415	0.005	1669.350	13.420	0.006
1668.345	13.229	0.004	1669.231	13.410	0.005	1669.352	13.429	0.007
1668.347	13.232	0.004	1669.237	13.422	0.005	1669.354	13.434	0.007
1668.352	13.227	0.005	1669.241	13.420	0.004	1669.357	13.437	0.009
1668.355	13.231	0.006						